

# “Raisin Bun”-Type Composite Spheres of Silica and Semiconductor Nanocrystals

Andrey L. Rogach,<sup>†,‡</sup> Dattatri Nagesha,<sup>†</sup> John W. Ostrander,<sup>†</sup>  
Michael Giersig,<sup>§</sup> and Nicholas A. Kotov<sup>\*,†</sup>

Department of Chemistry, Oklahoma State University, Stillwater, Oklahoma 74078,  
Physico-Chemical Research Institute, Belarusian State University, 220050 Minsk, Belarus, and  
Hahn-Meitner-Institut, Abt. Physikalische Chemie, Glienickestr. 100,  
D-15109, Berlin, Germany

Received March 20, 2000. Revised Manuscript Received June 27, 2000

CdTe nanocrystals capped with 1-mercapto-2,3-propanediol, CdSe nanocrystals capped with sodium citrate, and core-shell CdSe/CdS nanocrystals capped with sodium citrate were synthesized in aqueous solutions, and their surface was modified by 3-mercaptopropyltrimethoxysilane (MPS) in water-ethanol mixtures. By addition of sodium silicate, “raisin bun”-type composite particles were formed, with either CdTe, CdSe, or CdSe/CdS nanocrystals being homogeneously incorporated as multiple cores into silica spheres of 40–80 nm size, accompanied by some alteration of optical properties of the nanoparticles and, in particular, the reduction of the luminescence quantum yield. Further, growth of larger silica spheres (100–700 nm) can be performed by the Stöber technique using either MPS-modified semiconductor nanocrystals or “raisin bun”-type composite particles as seeds, which gives semiconductor-doped silica globules of desirable sizes in the submicrometer range. The composite spheres can be used as building blocks for 3D colloidal crystals, prepared in this study for CdS/CdSe-doped 250 nm silica colloid. The shift of the photonic band gap to the red was observed in photonic crystals made of nanoparticles-doped silica due to the high refractive index of the semiconductors.

## Introduction

Semiconductor nanocrystals prepared by wet chemical route are often considered for different applications, ranging from light-emitting diodes<sup>1–4</sup> to biological labels.<sup>5–7</sup> This interest arises from the possibility of tuning the optical properties of semiconductor nanocrystals by simply varying their size owing to the effect of quantum confinement.<sup>8</sup> The incorporation of metallic and semiconductor nanoparticles in the continuous solid films prepared by the sol-gel technique has led to inexpensive photonic materials partly already employed on the market or successfully tested with respect to numerous applications.<sup>9</sup> The new challenge in nanoparticle-based materials and corresponding optoelectronic applications is their 2D and 3D organization on

solid substrates. For nanocrystals taken as prepared, it was achieved by the Langmuir-Blodgett<sup>10</sup> or the layer-by-layer assembly techniques.<sup>11</sup> For nanoparticles

(9) Rottman, C.; Grader, G.; Hazan, Y. D.; Melchior, S.; Avnir, D. *J. Am. Chem. Soc.* **1999**, *121*, 8533–8543. Livage, J. *Bull. Mater. Sci.* **1999**, *22*, 201–205. Livage, J. *Mater. Sci. Forum* **1994**, *152–153*, 43–54. Livage, J.; Sanchez, C. *J. Non-Cryst. Solids* **1992**, *145*, 11–19. Patra, A.; Sominska, E.; Ramesh, S.; Koltypin, Y.; Zhong, Z.; Minti, H.; Reisfeld, R.; Gedanken, A. *J. Phys. Chem. B* **1999**, *103*, 3361–3365. Reisfeld, R.; Panczer, G.; Patra, A.; Gaft, M. *Mater. Lett.* **1999**, *38*, 413–417. Patra, A.; Reisfeld, R.; Minti, H. *Mater. Lett.* **1998**, *37*, 325–329. Lifshitz, E.; Dag, I.; Litvin, I.; Hodes, G.; Goror, S.; Reisfeld, R.; Zelman, M.; Minti, H. *Chem. Phys. Lett.* **1998**, *288*, 188–196. Zelman, M.; Minti, H.; Reisfeld, R.; Cohen, H.; Tenne, R. *Chem. Mater.* **1997**, *9*, 2541–2543. Zayat, M.; Einot, D.; Reisfeld, R. *J. Sol-Gel Sci. Technol.* **1997**, *10*, 67–74. Reisfeld, R. *Adv. Sci. Technol.* **1995**, *11*, 3–13. Sorek, Y.; Reisfeld, R.; Finkelstein, I.; Ruschin, S. *Opt. Mater. (Amsterdam)* **1994**, *4*, 99–101. Reisfeld, R. *Opt. Mater. (Amsterdam)* **1994**, *4*, 1–3. Sorek, Y.; Reisfeld, R.; Finkelstein, I.; Ruschin, S. *Appl. Phys. Lett.* **1993**, *63*, 3256–3258. Ptatschek, V.; Schreder, B.; Herz, K.; Hilbert, U.; Ossau, W.; Schottner, G.; Rahaeuser, O.; Bischof, T.; Lermann, G.; Materny, A.; Kiefer, W.; Bacher, G.; Forchel, A.; Su, D.; Giersig, M.; Mueller, G.; Spanhel, L. *J. Phys. Chem. B* **1997**, *101*, 8898–8906. Lembacher, C.; Schubert, U. *New J. Chem.* **1998**, *22*, 721–724. Kaiser, A.; Goersmann, A.; Schubert, U. *J. Sol-Gel Sci. Technol.* **1997**, *8*, 795–799. Schubert, U. *J. Chem. Soc., Dalton Trans.* **1996**, 3343–3348. Schubert, U.; Goersmann, C.; Schwertfeger, F.; Tewinkel, S. *Polym. Mater. Sci. Eng.* **1995**, *73*, 423–424. Schubert, U. *New J. Chem.* **1994**, *18*, 1049–1058. Schreder, B.; Schmidt, T.; Ptatschek, V.; Winkler, U.; Materny, A.; Umbach, E.; Lerch, M.; Mueller, G.; Kiefer, W.; Spanhel, L. *J. Phys. Chem. B* **2000**, *104*, 1677–1685. Leeb, J.; Gebhardt, V.; Mueller, G.; Haarer, D.; Su, D.; Giersig, M.; McMahon, G.; Spanhel, L. *J. Phys. Chem. B* **1999**, *103*, 7839–7845. Lorenz, C.; Emmerling, A.; Fricke, J.; Schmidt, T.; Hilgendorff, M.; Spanhel, L.; Muller, G. *J. Non-Cryst. Solids* **1998**, *238*, 1–5. Spanhel, L.; Schmidt, H.; Uhrig, A.; Klingshirn, C. *Mater. Res. Soc. Symp. Proc.* **1992**, *272*, 53–58. Spanhel, L.; Arpac, E.; Schmidt, H. *J. Non-Cryst. Solids* **1992**, *147–148*, 657–662. Spanhel, L.; Anderson, M. A. *J. Am. Chem. Soc.* **1991**, *113*, 2826–2833.

\* Corresponding author. E-mail: kotov@okstate.edu.

<sup>†</sup> Oklahoma State University.

<sup>‡</sup> Permanent address: Belarusian State University.

<sup>§</sup> Hahn-Meitner-Institut.

(1) Colvin, V. L.; Schlamp, M. C.; Alivisatos, A. P. *Nature* **1994**, *370*, 354.

(2) Gao, M. Y.; Richter, B.; Kirstein, S.; Möhwald, H. *J. Phys. Chem. B* **1998**, *102*, 4096.

(3) Mattoussi, H.; Radzilowski, L. H.; Dabbousi, B. O.; Thomas, E. L.; Bawendi, M. G.; Rubner, M. F. *J. Appl. Phys.* **1998**, *83*, 7965.

(4) Gaponik, N. P.; Talapin, D. V.; Rogach, A. L. *Phys. Chem. Chem. Phys.* **1999**, *1*, 1787.

(5) Bruchez, M.; Moronne, M.; Gin, P.; Weiss, S.; Alivisatos, A. P. *Science* **1998**, *281*, 2013.

(6) Chan, W. C. W.; Nie, S. *Science* **1998**, *281*, 2016.

(7) Mitchell, G. P.; Mirkin, C. A.; Letsinger, R. L. *J. Am. Chem. Soc.* **1999**, *121*, 8122.

(8) Weller, H. *Angew. Chem., Int. Ed.* **1993**, *32*, 41; Alivisatos, A. P. *J. Phys. Chem.* **1996**, *100*, 13226.

coated with silica, both the stability of the semiconductor core can be increased and a different periodicity of the nanoparticles arrangement can be obtained. Additionally, the silica surface can be easily modified with different groups to facilitate the solubility of spheres in different solvents and to control their interaction with substrate. While still pursuing other means of nanoparticles organization,<sup>10,11</sup> we focused this study on silica/semiconductor composite particles and synthesis of subsequent organization of quantum dots in the periodic crystalline structure with periodicity comparable to the wavelength of visible light.

An Individual coating of single nanoparticles with silica has been successfully realized for a variety of metal particles,<sup>12–14</sup> yielding silica spheres of the desired sizes containing a single metal core placed precisely at their centers. Coating of small 4–10 nm single semiconductor nanocrystals with silica has been realized and has been shown to suppress the photochemical degradation of the nanoparticles.<sup>5,15</sup> On the other hand, doping of 50–1000 nm uniformly sized silica colloids with luminescent semiconductor nanocrystals has not yet been realized. Optically active SiO<sub>2</sub> colloids can serve as the starting point for a variety of photonic materials such as laser media, diffraction gratings, and sensing films. As well, such particles are needed for the investigation of fundamental particle–particle interactions in fluid media, which despite a quite long history, continue to surprise the researchers.<sup>16</sup> In this respect, the silica spheres doped with luminescent semiconductor nanoparticles can be used for monitoring of the

colloidal motion in solution by confocal microscopy. Currently, luminescence tagging is usually achieved by incorporating dyes in the colloidal particles,<sup>17</sup> which undergo fast photobleaching.

A large class of photonic materials is based on monodisperse silica—the so-called artificial opals. They are attracting much attention recently due to their unique optical properties and their causative similarity to the electrical properties of solids.<sup>18–27</sup> Colloidal crystals prepared by the self-organization of monodisperse latex<sup>28,29</sup> or silica<sup>28,23–25,30–32</sup> spheres have been shown to possess a photonic pseudogap and, therefore, are considered as promising prototypes for 3D photonic crystals ("optical semiconductors") in the visible and near-IR parts of the electromagnetic spectrum. These findings have stimulated extensive studies of the structural<sup>22,24,27,30–33</sup> and optical<sup>22,24,30,32</sup> properties of colloidal crystals, their use as templates for fabricating high-refractive index 3D replicas,<sup>34</sup> and the spontaneous emission of dye molecules<sup>35</sup> and semiconductor nanocrystals<sup>36–39</sup> embedded into the voids of colloidal crys-

- (10) Kotov, N. A.; Meldrum, F. C.; Fendler, J. H. *J. Phys. Chem.* **1994**, *98*, 8827. Kotov, N. A.; Meldrum, F. C.; Wu, C.; Fendler, J. H. *J. Phys. Chem.* **1994**, *98*, 2735–2738. Meldrum, F. C.; Kotov, N. A.; Fendler, J. H.; *Langmuir* **1994**, *10*, 2035–2040. Meldrum, F. C.; Kotov, N. A.; Fendler, J. H. *Chem. Mater.* **1995**, *7*, 1112–1116. Meldrum, F. C.; Kotov, N. A.; Fendler, J. H. *J. Chem. Soc., Faraday Trans.* **1995**, *91* (4), 673–680. Markovich, G.; Collier, C. P.; Heath, J. R. *Phys. Rev. Lett.* **1998**, *80*, 3807–3810. Medeiros-Ribeiro, G.; Ohlberg, D. A. A.; Williams, R. S.; Heath, J. R. *Phys. Rev. B: Condens. Matter Mater. Phys.* **1999**, *59*, 1633–1636. Henrichs, S. E.; Sample, J. L.; Shiang, J. J.; Heath, J. R.; Collier, C. P.; Saykally, R. J. *J. Phys. Chem. B* **1999**, *103*, 3524–3528. Weitz, I. S.; Sample, J. L.; Ries, R.; Spain, E. M.; Heath, J. R. *J. Phys. Chem. B* **2000**, *104*, 4288–4291. Dabbousi, B. O.; Murray, C. B.; Rubner, M. F.; Bawendi, M. G. *Chem. Mater.* **1994**, *6*, 216–219. Fendler, J. H. *Chem. Mater.* **1996**, *8*, 1616–1624. Li, L. S.; Hui, Z.; Chen, Y.; Zhang, X. T.; Peng, X.; Liu, Z.; Li, T. J. *J. Colloid Interface Sci.* **1997**, *192*, 275–280.
- (11) Kotov, N. A.; Fendler, J. H.; Dekany, I. *J. Phys. Chem.* **1995**, *99*, 13065. Aliev, F.; Correa-Duarte, M. A.; Mamedov, A.; Ostrander, J. W.; Giersig, M.; Liz-Marzan, L. M.; Kotov, N. A. *Adv. Mater.* **1999**, *11* (12), 1006–1010. Mamedov, A.; Ostrander, J. W.; Aliev, F.; Kotov, N. A. *Langmuir* **2000**, *16* (8), 3941–3949. Pastoriza-Santos, I.; Koktysh, D. S.; Mamedov, A. A.; Giersig, M.; Kotov, N. A.; Liz-Marzan, L. M. *Langmuir* **2000**, *16* (6), 2731–2735. Mamedov, A.; Kotov, N. A. *Langmuir* **2000**, *16*, 5530. Rogach, A.; Koktysh, D.; Harrison, M.; Kotov, N. A. *Chem. Mater.* **2000**, *12*, 1526. Liu, Y. J.; Wang, A. B.; Claus, R. O. *Appl. Phys. Lett.* **1997**, *71*, 2265–2267. Lvov, Y.; Ariga, K.; Onda, M.; Ichinose, I.; Kunitake, T. *Langmuir* **1997**, *13*, 6195–6203. Caruso, F.; Lichtenfeld, H.; Giersig, M.; Mohwald, H. *J. Am. Chem. Soc.* **1998**, *120*, 8523–8524. Decher, G.; Schmitt, J.; Brand, F.; Lehr, B.; Oeser, R.; Losche, M.; Bouwman, W.; Kjaer, K.; Calvert, J.; Geer, R.; Dressik, W.; Shashidhar, R. *Adv. Mater.* **1998**, *10*, 338. Gao, M. Y.; Richter, B.; Kirstein, S.; Möhwald, H. *J. Phys. Chem. B* **1998**, *102*, 4096. Gao, M. Y.; Kirstein, S.; Rogach, A. L.; Weller, H.; Möhwald, H. *Adv. Sci. Technol. (Faenza, Italy)* **1999**, *27*, 347.
- (12) (a) Liz-Marzán, L. M.; Giersig, M.; Mulvaney, P. *Chem. Commun.* **1996**, 731. (b) Buining, P. A.; Liz-Marzán, L. M.; Philipse, A. P. *J. Colloid Interface Sci.* **1996**, *179*, 318.
- (13) Liz-Marzán, L. M.; Giersig, M.; Mulvaney, P. *Langmuir* **1996**, *12*, 4329.
- (14) Ung, T.; Liz-Marzán, L. M.; Mulvaney, P. *Langmuir* **1998**, *14*, 3740.
- (15) Correa-Duarte, M. A.; Giersig, M.; Liz-Marzán, L. M. *Chem. Phys. Lett.* **1998**, *286*, 497.
- (16) Aranda-Espinoza, H.; Chen, Yi.; Dan, N.; Lubensky, T. C.; Nelson, P.; Ramos, L.; Weitz, D. A. *Science* **1999**, *285*, 394. Ramos, L.; Lubensky, T. C.; Dan, N.; Nelson, P.; Weitz, D. A. *Science* **1999**, *286*, 2325. Wei, Q.-H.; Bechinger, C.; Leiderer, P. *Science* **1999**, *287*, 625. Weeks, E. R.; Crocker, J. C.; Levitt, A. C.; Schofield, A.; Weitz, D. A. *Science* **1999**, *287*, 627.
- (17) Char, K.; Frank, C. W.; Gast, A. P. *Langmuir* **1990**, *6*, 767. Koppel, D. E.; Morgan, F.; Cowan, A. E.; Carson, J. H. *Biophys. J.* **1994**, *66*, 502. Lowe, C. P.; Frenkel, D. *Phys. Rev. E* **1996**, *54*, 2704.
- (18) Jiang, P.; Bertone, J. F.; Hwang, K. S.; Colvin, V. L. *Chem. Mater.* **1999**, *11*, 2132.
- (19) Tarhan, I. I.; Watson, H. *Phys. Rev. Lett.* **1996**, *76*, 315.
- (20) Vos, W. L.; Sprik, R.; van Blaaderen, A.; Imhof, A.; Lagendijk, A.; Wegdam, G. H. *Phys. Rev. B* **1996**, *53*, 16231.
- (21) Astratov, V. N.; Vlasov, Yu. A.; Karimov, O. Z.; Kaplyanski, A. A.; Musikhin, Yu. G.; Bert, N. A.; Bogomolov, V. N.; Prokofiev, A. V. *Phys. Lett. A* **1996**, *222*, 349.
- (22) Bogomolov, V. N.; Gaponenko, S. V.; Germanenko I. N.; Kapitonov, A. M.; Petrov, E. P.; Gaponenko, N. V.; Prokofiev, A. V.; Pomyavina, A. N.; Silvanovich, N. I.; Samoilovich, S. M. *Phys. Rev. E* **1997**, *55*, 7619.
- (23) Van Blaaderen, A.; Ruel, R.; Wiltzius, P. *Nature* **1997**, *385*, 321.
- (24) Miguez, H.; Lopez, C.; Meseguer, F.; Blanco, A.; Vazquez, L.; Mayoral, R.; Ocana, M.; Fornes, V.; Mifsud, A. *Appl. Phys. Lett.* **1997**, *71*, 1148.
- (25) Van Blaaderen, A. *Science* **1998**, *282*, 887.
- (26) Romanov, S. G.; Fokin, A. V.; de la Rue, R. M. *J. Phys. C* **1999**, *11*, 3593.
- (27) Rogach, O. E.; Kornowski, A.; Kapitonov, A. M.; Gaponenko, N. V.; Gaponenko, S. V.; Eychemüller, A.; Rogach, A. L. *Mater. Sci. Eng. B* **1999**, *64*, 64.
- (28) Pieranski, P. *Contemp. Phys.* **1983**, *24*, 25.
- (29) Clark, N. A.; Hurd, A. J.; Ackerson, B. J. *Nature* **1979**, *281*, 57. Tarhan, I. I.; Zunkin, M. P.; Watson, G. H. *Opt. Lett.* **1995**, *20*, 1571. Fujimura, T.; Edamatsu, K.; Itoh, T.; Shimada, R.; Imada, A.; Koda, T.; Chiba, N.; Muramatsu, H.; Ataka, T. *Opt. Lett.* **1997**, *22*, 489. Park, S. H.; Gates, B.; Xia, Y. *Adv. Mater.* **1999**, *11*, 462. Gates, B.; Qin, D.; Xia, Y. *Adv. Mater.* **1999**, *11*, 466.
- (30) Jiang, P.; Hwang, K. S.; Mittleman, D. M.; Bertone, J. F.; Colvin, V. L. *J. Am. Chem. Soc.* **1999**, *121*, 11630–11637. Jiang, P.; Cizeron, J.; Bertone, J. F.; Colvin, V. L. *J. Am. Chem. Soc.* **1999**, *121*, 7957–7958. Tsunekawa, S.; Barnakov, Y.; Poborchii, V. V.; Samoilovich, S. M.; Kasuya, A.; Nishina, Y. *Microporous Mater.* **1997**, *8*, 275–282. Hayward, R. C.; Saville, A.; Aksay, A. *Nature (London)* **2000**, *404*, 56–59.
- (31) Mayoral, R.; Requena, J.; Moya, J. S.; Lopez, C.; Cintas, A.; Miguez, H.; Meseguer, F.; Vazquez, L.; Holgado, M.; Blanco, A. *Adv. Mater.* **1997**, *9*, 257. Miguez, H.; Meseguer, F.; Lopez, C.; Mifsud, A.; Moya, J. S.; Vazquez, L. *Langmuir* **1997**, *13*, 6009.
- (32) Bogomolov, V. N.; Gaponenko, S. V.; Kapitonov, A. M.; Prokofiev, A. V.; Pomyavina, A. N.; Silvanovich, N. I.; Samoilovich, S. M. *Appl. Phys. A* **1996**, *63*, 613. Miguez, H.; Meseguer, F.; Lopez, C.; Blanco, A.; Moya, J. S.; Requena, J.; Mifsud, A.; Fornes, V. *Adv. Mater.* **1998**, *10*, 480. Vlasov, Yu. A.; Astratov, V. N.; Karimov, O. Z.; Kaplyanski, A. A.; Bogomolov, V. N.; Prokofiev, A. V. *Phys. Rev. B* **1997**, *55*, 13357.
- (33) Megens, M.; van Kats, C. M.; Bösecke, P.; Vos, W. L. *J. Appl. Crystallogr.* **1997**, *30*, 637. Vos, W. L.; Megens, M.; van Kats, C. M.; Bösecke, P. *Langmuir* **1997**, *13*, 6004.



tals. Because of the substantial difference between the electron and photon wavelengths, the electron and photon densities of states can be engineered separately within the same mesoscopic structure, which can be realized in colloidal photonic crystals doped with luminescent semiconductor nanocrystals.<sup>36–39</sup> The interplay of electron and photon confinement opens the pathway to novel light sources with controllable spontaneous emission.

In this paper, we report the synthesis of “raisin-bun”-type submicrometer-size composite spheres of silica labeled with different semiconductor nanocrystals: thiol-capped CdTe nanoparticles, citrate-stabilized CdSe nanoparticles, and citrate-stabilized core–shell CdSe/CdS nanocrystals. The optical properties of photonic crystal with quantum dots positioned inside silica spheres are principally different from the approaches reported in refs 36–39, where nanocrystals were infiltrated in voids. Besides the protection from oxidation, embedding the nanoparticles in the core of the colloid has significant advantage over adsorbing the nanoparticles on the surface,<sup>40</sup> because this does not alter particle–particle interactions and affords further functionalization of silica. The isolation of the nanoparticles inside the spheres allows for decoupling of the media effects on photonic band gap and media effects on the luminescence intensity of quantum dots, which will interfere otherwise. This feature combined with the controllable diameter of silica spheres and the variable emission of spectrum of nanoparticles makes possible the comprehensive study of the interplay between the photonic and electronic characteristics. We successfully realized the encapsulation of spatially separated quantum dots inside the silica spheres. However, the simultaneous decrease of the luminescence quantum yield was observed for all nanoparticles used in this study. This problem is quite important in the context of possible photonic applications and will require further experimental work. On the other hand, the incorpora-

tion of the nanocrystals altered the photonic band gap of the colloidal crystal, which demonstrated the possibility of the band gap tuning independently of the silica sphere diameter and void medium.

## Experimental Section

For the preparation of composite silica structures, sodium silicate solution (27 wt % SiO<sub>2</sub>, Fisher Scientific), 3-mercaptopropyltrimethoxysilane (MPS, Fluka), tetraethoxysilane (TEOS, 98%, Fluka), and pure grade ethanol were used as received. Milli-Q-deionized water was used for all the preparations.

Aqueous solutions of CdTe nanocrystals capped with 1-mercapto-2,3-propanediol (thioglycerol) were prepared by the method of Rogach et al. reported previously.<sup>41</sup> Briefly, 22 mL of freshly prepared oxygen-free 0.05 M NaHTe solution was added to 125 mL of a 0.013 M nitrogen-saturated Cd(ClO<sub>4</sub>)<sub>2</sub>·6H<sub>2</sub>O aqueous solution at pH 11.2 in the presence of 0.5 mL of 1-thioglycerol as a stabilizing agent. The solution was heated to 96 °C and refluxed for as long as 48 h to promote the growth of CdTe nanocrystals. Fractions of CdTe nanoparticles of different sizes were taken from the crude solution at different reflux times, precipitated by 2-propanol, redissolved in pure water again at pH 9.0, and used for preparation of composite structures.

Citrate-stabilized CdSe nanocrystals were prepared according to the following procedure: To 45 mL of water were added 0.05 g sodium citrate and 2 mL of  $4 \times 10^{-2}$  M cadmium perchlorate and the pH was adjusted to 9.0 by 0.1 M NaOH. The solution was bubbled with nitrogen for 10 min, 2 mL of  $1 \times 10^{-2}$  M *N,N*-dimethylselenourea was added, and the mixture was heated in a conventional 900 W (Sharp) microwave oven for 50 s. The final volume of the solution after heating was ca. 40 mL. In the recipe described above, the Cd:Se molar ratio was 4:1, which leads to CdSe nanoparticles with ca. 4.0 nm diameter; by increasing the Cd concentration it is possible to synthesize smaller CdSe nanocrystals.

For the preparation of core–shell CdSe/CdS nanocrystals, citrate-stabilized CdSe nanoparticles synthesized in aqueous solution as described above (Cd:Se molar ratio 4:1) were used as the initial material with thioacetamide as a sulfur source. To a given volume of CdSe nanoparticle solution as prepared was added a  $4 \times 10^{-2}$  M solution of thioacetamide in a quantity that the molar ratio of S<sub>added</sub>:S<sub>initial</sub> was 1:1. The mixture was heated in the sealed round-bottom flask in a silicon oil bath at 70–80 °C for up to 24 h.

Composite structures of silica and semiconductor nanocrystals were prepared by the modified method of ref 15. First, a solution of 2 μL of MPS in 80 mL of ethanol was added under vigorous stirring to 20 mL of aqueous solutions of CdTe, CdSe, or CdSe/CdS nanocrystals with a nanoparticle concentration of 0.5 and 1.5 mM referred to Cd for CdTe and CdSe/CdS nanoparticles, respectively. The mixtures were stirred for ca. 12 h and then 0.4 mL of 0.54 wt % solution of sodium silicate was added to 40 mL of these solutions. The addition of silicate resulted in a pH increase from 8.5 to 10.7. The mixtures were allowed to react for about 4 h under UV–vis control and then ripened for 5 days.

Silica spheres doped with semiconductor nanocrystals were prepared by the modified Stöber synthesis<sup>42</sup> using ethanol–water mixtures of either MPS-modified semiconductor nanocrystals or “raisin bun”-type composite particles as growth seeds.

Colloidal crystals were made by slow natural sedimentation of charge-stabilized nanocrystal-doped silica spheres from DMF, followed by evaporation of the solvent.<sup>27</sup>

(34) Norris, D. J. *Adv. Mater.* **1999**, *11*, 165. Park, S. H.; Xia, Y. *Adv. Mater.* **1998**, *10*, 1045. Park, S. H.; Xia, Y. *Chem. Mater.* **1998**, *10*, 1745. Holland, B. T.; Blanford, C. F.; Stein, A. *Science* **1998**, *281*, 538. Wijnhoven, J. E. G. J.; Vos, W. L. *Science* **1998**, *281*, 802. Zakhidov, A. A.; Baughman, R. H.; Iqbal, Z.; Cui, C.; Khayrullin, I.; Dantas, S. O.; Marti, J.; Ralchenko, V. G. *Science* **1998**, *282*, 897. Kapitonov, A. M.; Gaponenko, N. V.; Bogomolov, V. N.; Prokofiev, A. V.; Samoilovich, S. M.; Gaponenko, S. V. *Phys. Stat. Solidi (a)* **1998**, *165*, 119. Vlasov, Yu. A.; Yao, N.; Norris, D. J. *Adv. Mater.* **1999**, *11*, 165.

(35) Petrov, E. P.; Bogomolov, V. N.; Kalosha, I. I.; Gaponenko, S. V. *Phys. Rev. Lett.* **1998**, *81*, 77. Yamasaki, T.; Tsutsui, T. *Appl. Phys. Lett.* **1998**, *72*, 1957. Yoshino, K.; Tada, K.; Ozaki, M.; Zakhidov, A. A.; Baughman, R. H. *Appl. Phys. Lett.* **1998**, *73*, 3506.

(36) Vlasov, Yu. A.; Luterova, K.; Pelant, I.; Hönerlage, B.; Astratov, V. N. *Appl. Phys. Lett.* **1997**, *71*, 1616. Astratov, V. N.; Bogomolov, V. N.; Kaplyanskiy, A. A.; Prokofiev, A. V.; Samoilovich, L. A.; Samoilovich, S. M.; Vlasov, Yu. A. *Nuovo Cimento D* **1995**, *17*, 1349. Vlasov, Yu. A.; Yao, N.; Norris, D. J. *Adv. Mater.* **1999**, *11*, 165.

(37) Blanco, A.; Lopez, C.; Mayoral, R.; Meseguer, F.; Mifsud, A.; Herrero, J. *Appl. Phys. Lett.* **1998**, *73*, 1781. Miguez, H.; Blanco, A.; Lopez, C.; Meseguer, F.; Yates, H. M.; Pemble, M. E.; Lopez-Tejiera, F.; Garcia-Vidal, F. J.; Sanchez-Dehesa, J. *J. Lightwave Techn.* **1999**, *17*, 1975.

(38) Romanov, S. G.; Fokin, A. V.; Alperovich, V. I.; Johnson, N. P.; De La Rue, R. M. *Phys. Stat. Solidi (a)* **1997**, *164*, 169.

(39) Gaponenko, S. V.; Kapitonov, A. M.; Bogomolov, V. N.; Prokofiev, A. V.; Eychmüller, A.; Rogach, A. L. *JETP Lett.* **1998**, *68*, 142.

(40) Susha, A. S.; Caruso, F.; Rogach, A. L.; Sukhorukov, G. B.; Kornowski, A.; Möhwald, H.; Giersig, M.; Eychmüller, A.; Weller, H. *Colloid. Surf. A* **2000**, *163*, 39. Megens, M.; Wijnhoven, J. E. G. J.; Lagendijk, A.; Vos, W. L. *J. Opt. Soc. Am. B* **1999**, *16*, 1403. Megens, M.; Wijnhoven, J. E. G. J.; Lagendijk, A.; Vos, W. L. *Phys. Rev. A* **1999**, *59*, 4727.

(41) Rogach, A. L.; Katsikas, L.; Kornowski, A.; Su, D.; Eychmüller, A.; Weller, H. *Ber. Bunsen-Ges. Phys. Chem.* **1996**, *100*, 1772; **1997**, *101*, 1668.

(42) Stöber, W.; Fink, A.; Bohn, E. *J. Colloid Interface Sci.* **1968**, *26*, 62.

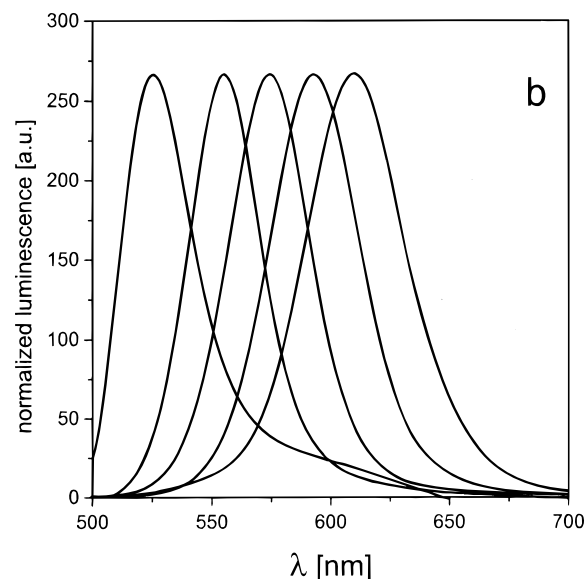
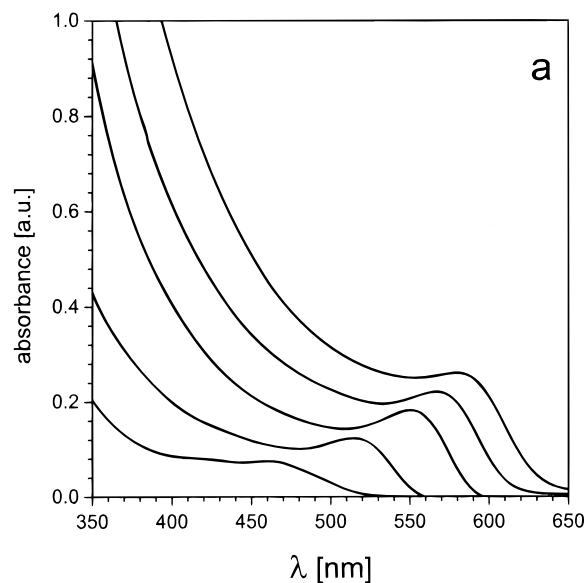


**Figure 1.** Absorption (a) and luminescence (b) spectra of thioglycerol-capped CdTe nanocrystals of different sizes (2.5–5.0 nm) in aqueous solutions.

UV–vis absorption spectra were taken on a HP8453 diode array Hewlett-Packard spectrophotometer. Photoluminescence spectra were measured on a modular Fluorolog 3 SPEX spectrofluorimeter. Transmission electron microscopy (TEM) images were taken on a Philips CM12 microscope operating at an acceleration voltage of 120 kV and on a Philips CM200 FEG microscope operating at an acceleration voltage of 200 kV. High-resolution TEM images were digitally recorded with a CCD camera. Samples were prepared by evaporation of a drop of colloidal solution on a carbon-coated copper grid. Scanning electron microscopy (SEM) pictures were made with a JSM 6400 microscope.

## Results

**Preparation of Nanocrystals.** Thioglycerol-capped CdTe nanoparticles show a peak corresponding to 1s–1s electronic transitions in the absorption spectra (Figure 1a) and a pronounced, relatively narrow (fwhm = 35–50 nm) "excitonic" luminescence (5% room-temperature quantum efficiency as measured in comparison with Rhodamine 6G), which is tunable with particle size

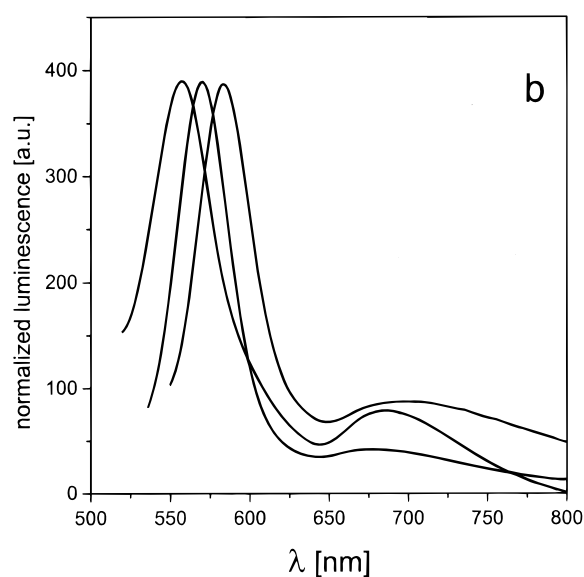
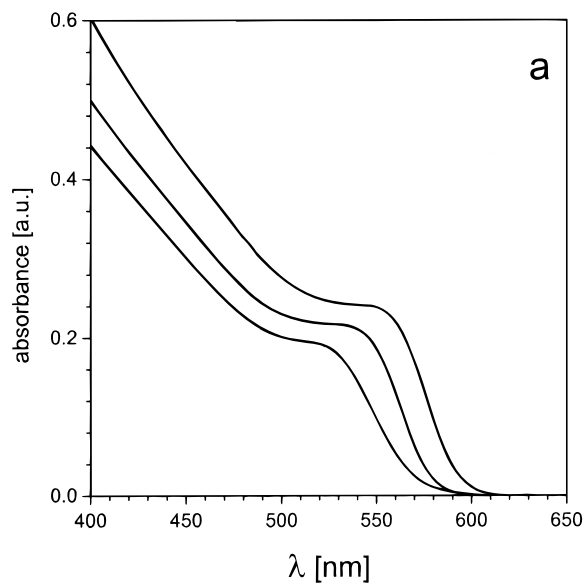


**Figure 2.** Absorption (a) and luminescence (b) spectra of citrate-stabilized CdSe nanocrystals of different sizes (3.0–5.0 nm) in aqueous solutions.

due to the quantum confinement effect (Figure 1b). There is also a weak luminescence band originating from the emission from trap sites<sup>43</sup> that is strongly redshifted from the absorption onset and is more pronounced in smaller CdTe nanoparticles. Particles grow continuously during the prolonged refluxing from ca. 2.5 to 5.0 nm. It is envisaged that thiols slowly decomposed during reflux and serve as a sulfide source, so the formation of mixed and core–shell CdTe/CdS crystals particles is likely for advanced stages of heating.<sup>44</sup>

Citrate-stabilized CdSe nanocrystals also show well-defined 1s–1s electronic transitions in the absorption spectra (Figure 2a), excitonic emission that are tunable with particle size in the visible spectral region, albeit not to such an extent as for thiol-capped CdTe nanocrystals, and relatively strong trapped emission (Figure 2b). The room-temperature excitonic emission of CdSe

(43) Kapitonov, A. M.; Stupak, A. P.; Gaponenko, S. V.; Petrov, E. P.; Rogach, A. L.; Eychmüller, A. *J. Phys. Chem. B* **1999**, *103*, 10109.

(44) Rogach, A. L. *Mater. Sci. Eng. B*, **2000**, *69*, 435.

nanoparticles is weak, ca. 0.1–0.15% in comparison with Rhodamine 6G. However, the useful feature of nanoparticles synthesized with citrate is the combination of a relatively narrow size distribution and lability of the stabilizer, which is beneficial for many reactions of the excitonic luminescence. The quantum efficiency of the excitonic luminescence can be sufficiently enhanced by capping the surface of the nanocrystals with a higher band gap inorganic layer. These "core/shell" composite materials show sufficiently higher luminescence quantum yield than "bare" nanoparticles due to improved passivation of the surface. Examples of such core/shell structures include CdSe/ZnSe,<sup>45</sup> CdSe/ZnS,<sup>46,47</sup> and CdSe/CdS<sup>48</sup> nanoparticles synthesized by the TOP/TOPO method, with reports of room-temperature quantum efficiencies of up to 50% for the CdSe/CdS material.<sup>48</sup> It was therefore decided to overcoat our CdSe nanocrystals with a layer of CdS in order to obtain a material with higher luminescence quantum yield. Thioacetamide was chosen as a sulfur source as it can gradually liberate sulfide ions in aqueous solution, which slowly react with excess of Cd<sup>2+</sup> in the CdSe colloidal solution.<sup>49</sup>

In the course of the preparation of the core-shell particles, both absorption and luminescent spectra of CdSe undergo some change as compared to mere heating without the sulfur source (Figure 3). The heating induces a slight growth of CdSe nanocrystals that is accompanied by the red shift of the absorption edge and excitonic luminescence band (compare Figures 2 and 3). For CdSe/CdS nanoparticles, absorbance increases at all wavelengths, and the absorption edge shifts 3–4 nm to the red. The luminescence maximum of excitonic band shifts correspondingly by 4–5 nm to the red, and the relative intensity of trapped emission decreases, while its maximum shifts by 20 nm to the blue. The luminescence intensity grows up drastically—20–30 times—and the quantum yield reaches 4.2%. Note that the luminescence intensity of bare CdSe particles, when heated, increases as well; however, the quantum yield in this case never exceeded 0.5–0.8%. This indicates the formation of CdS shells on CdSe cores, which passivates CdSe surface defects and leads to the localization of photoexcited charge carriers in the CdSe core. Correspondingly, the trapped emission of bare CdSe nanoparticles is strongly depressed for the CdSe/CdS core-shells, whereas the relative intensity of trapped emission of bare CdSe nanoparticles increases during heating. Note that the presence of the epitaxially deposited CdS shell cannot be seen in the TEM images even at the highest resolution, because the crystal structures of hexagonal CdS and CdSe are very close, and therefore, one has to limit the probing of the core-shell structures to spectroscopic means.

**Silication of the Nanocrystals.** CdTe nanocrystals capped with thioglycerol, CdSe nanocrystals capped

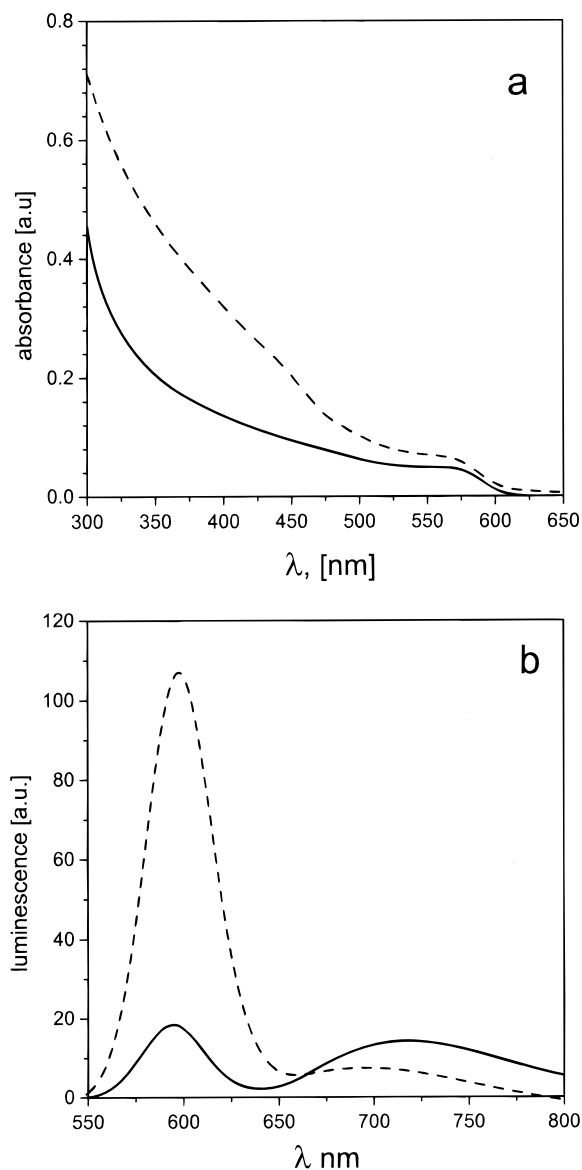


**Figure 3.** Absorption (a) and luminescence (b) spectra of "bare" CdSe nanoparticles (solid lines) and CdSe/CdS nanoparticles (dashed lines). Both samples were heated in the silicon oil bath at 70 °C for 24 h.

with sodium citrate, and core-shell CdSe/CdS nanocrystals capped with sodium citrate were used for the preparation of composite structures with silica. The average size of the nanoparticles used was 3.0, 4.0, and 5.0 nm for CdTe, CdSe, and CdSe/CdS, respectively, with ca. 15% polydispersity.

Morphological changes occurring during the modification of nanocrystals with MPS and silicate have been followed by TEM (Figure 4). Unmodified nanocrystals tend to form agglomerates on the TEM grids when the solvent is evaporated (Figure 4a). No formation of silica shells has been observed for nanocrystals whose surface is modified by MPS, although they appear to be more isolated on TEM images (Figure 4b) than unmodified ones, probably because of stronger steric and electrostatic repulsion. After addition of silicate, SiO<sub>2</sub> spheres 40–80 nm in diameter are formed (Figure 4c) in colloidal solution, with semiconductor nanocrystals being incorporated in silica as multiple cores (Figure 4d).

(45) Danek, M.; Jensen, K. F.; Murray, C. B.; Bawendi, M. G. *Chem. Mater.* **1996**, *8*, 173.

(46) Hines, M. A.; Guyot-Sionnest, P. *J. Phys. Chem.* **1996**, *100*, 468.

(47) Dabbousi, B. O.; Rodriguez-Viejo, J.; Mikulec, F. V.; Heine, J. R.; Mattoussi, H.; Ober, R.; Jensen, K. F.; Bawendi, M. G. *J. Phys. Chem. B* **1997**, *101*, 9463.

(48) Peng, X.; Schlamp, M. C.; Kadavanich, A. V.; Alivisatos, A. P. *J. Am. Chem. Soc.* **1997**, *119*, 7019.

(49) Li, Y.; Xu, D.; Zhang, Q.; Chen, D.; Huang, F.; Xu, Y.; Guo, G.; Gu, Z. *Chem. Mater.* **1999**, *11*, 3433.



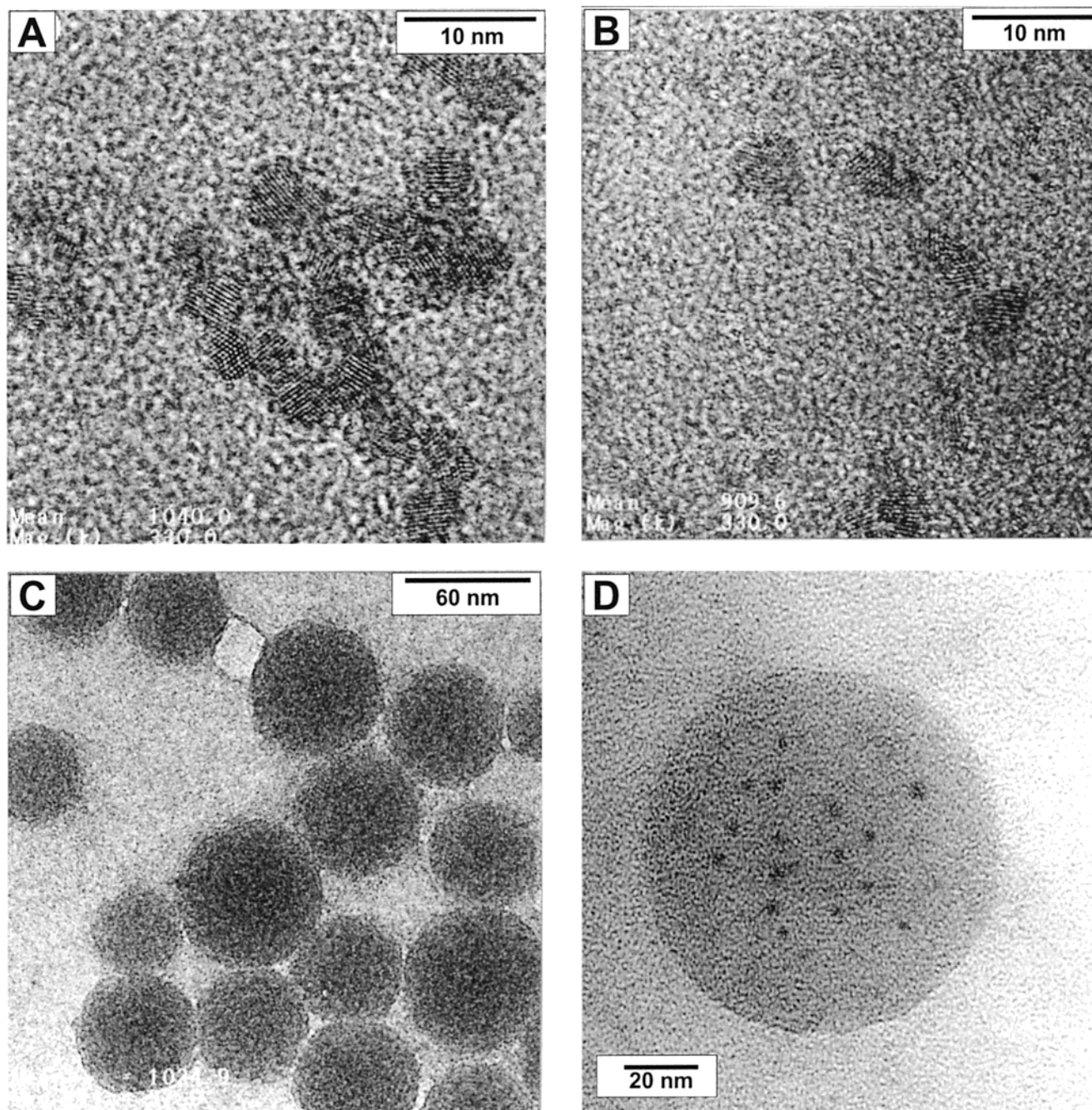


**Figure 4.** TEM images illustrating morphological changes during modification of nanocrystals: (a) CdSe nanocrystals from the original aqueous dispersion; (b) CdSe nanoparticles modified by MPS; (c) silica spheres (with inclusions of CdSe nanocrystals) which were formed after silicate addition; (d) an enlarged view of a silica sphere with inclusions of CdTe nanocrystals.

Figures 5 and 6 show absorption and luminescence spectra of selected samples of CdTe and CdSe/CdS nanocrystals in aqueous solutions as prepared and of the same nanoparticles modified with MPS and silicate as described in the Experimental Section. After addition of MPS, the maximum in the absorption spectra of CdTe nanocrystals corresponding to the first electronic transition becomes less pronounced and shifts to shorter wavelengths by ca. 10 nm (Figure 5a); a concomitant 9 nm blue shift is observed for the excitonic band of CdTe nanocrystals in the luminescence spectrum (Figure 5b). Almost no change is observed in both absorption and photoluminescence spectra of CdSe/CdS nanoparticles after the modification with MPS. After addition of silicate, the maximum in the absorption spectrum

becomes broader and less pronounced for both CdTe and CdSe/CdS nanocrystals (Figures 5a, 6a); for CdTe nanoparticles it shifts further to shorter wavelengths. Correspondingly, the excitonic luminescence band of CdTe nanoparticles shifts further to shorter wavelengths and becomes broader, and luminescence from traps becomes more pronounced (Figure 5b). The excitonic luminescence band of CdSe/CdS nanoparticles after addition of silicate remains nearly at the same wavelengths as for unmodified CdSe/CdS nanocrystals but becomes sufficiently broader, and emission from traps becomes stronger (Figure 6b), which hints at the existence of "holes" in the CdS epitaxial coat. The luminescence intensity decreases strongly (about 20 times) after

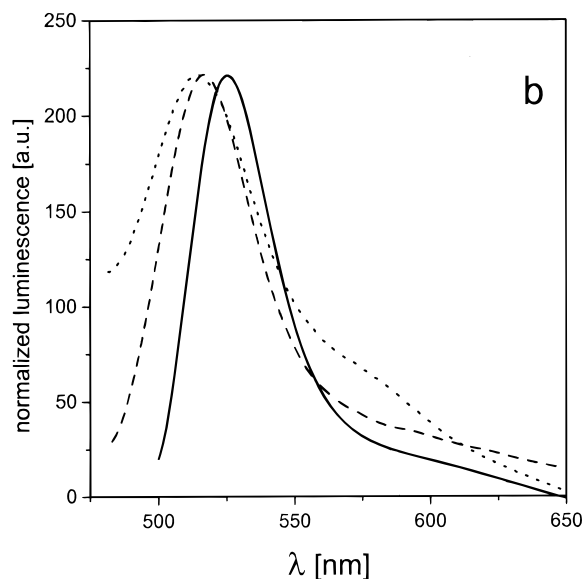
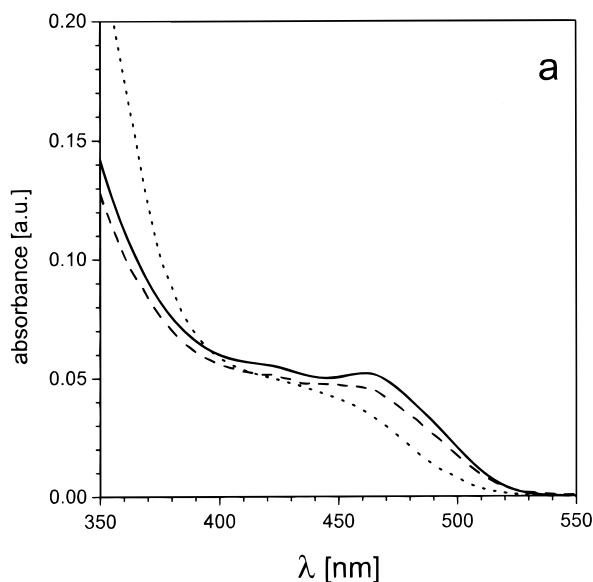


**Figure 5.** Absorption (a) and luminescence (b) spectra of unmodified CdTe nanocrystals (solid lines), CdTe nanocrystals modified with MPS (dashed lines) and composite CdTe@SiO<sub>2</sub> spheres formed after silicate addition (dotted lines).

silicate addition to both CdTe and CdSe/CdS nanoparticles, in comparison with unmodified nanocrystals.

Changes in absorption and luminescence spectra observed for the citrate-stabilized CdSe nanocrystals due to MPS and silicate modification repeat those for CdSe/CdS nanoparticles. Luminescence of MPS- and silicate-modified bare CdSe nanocrystals, being weak enough for unmodified CdSe nanocrystals, almost completely disappears, while the CdSe/CdS core–shells still show noticeable luminescence.

The further growth of silica spheres from 40 to 80 nm in diameter (Figure 4c) to 200–400 nm, for which the photonic band gap effects can be observed in the visible region, can be performed by the Stöber technique<sup>42</sup> using either MPS-modified semiconductor nanocrystals or “raisin bun”-type composite particles as seeds. This process yields silica globules in the range of 100–700 nm, which is quite convenient for further studies.<sup>27</sup> Figure 7 shows a TEM image of silica globules of 250

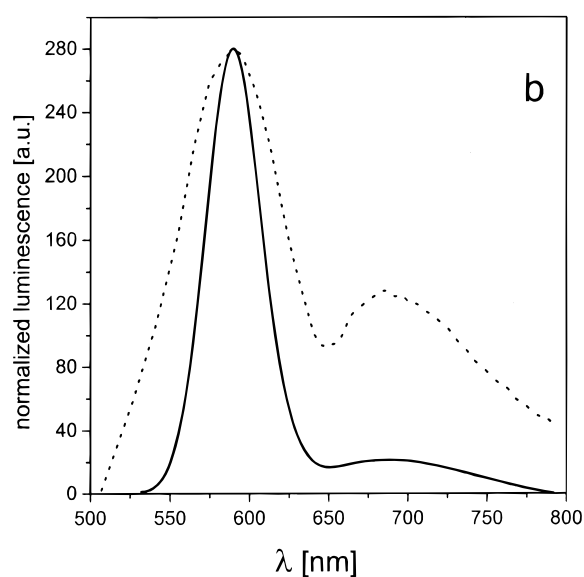
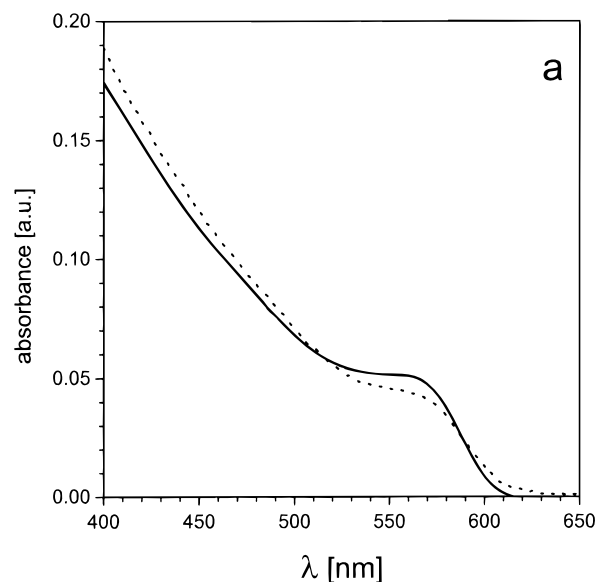


**Figure 6.** Absorption (a) and luminescence (b) spectra of unmodified CdSe/CdS nanocrystals (solid lines) and composite CdSe/CdS@SiO<sub>2</sub> spheres formed after silicate addition (dotted lines). Absorption and photoluminescence spectra of CdSe/CdS nanoparticles modified with MPS are almost the same as for unmodified CdSe/CdS nanocrystals and are not shown here.

nm size synthesized by the modified Stöber method with MPS-modified CdSe/CdS semiconductor particles as seeds for the silica growth. Composite particles formed have yellowish color because of the CdSe/CdS doping. Unfortunately, large diameter of the colloid made it impossible to view semiconductor nanocrystals incorporated in large silica spheres with a transmission electron microscope. “Raisin bun”-type composite particles can be used as seeds in the Stöber synthesis as well, giving structures with a thick silica shell and a 40–80 nm core where semiconductor nanocrystals are to be confined.

**Colloidal Crystals Made from Doped Silica Spheres.** When allowed to sediment, charge-stabilized submicrometer-size silica spheres can organize themselves into a 3D regular lattice.<sup>28–39,50</sup> Similarly, evaporation of the solvent from the nanoparticle-doped SiO<sub>2</sub> leads to colloidal crystals. Figure 8 shows a SEM picture



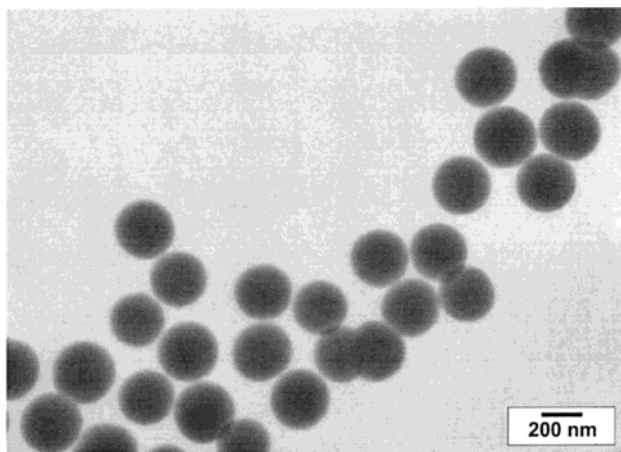


**Figure 7.** TEM image of silica globules of 250 nm size synthesized by the modified Stöber method with MPS-modified CdSe/CdS semiconductor particles as seeds for the silica growth.

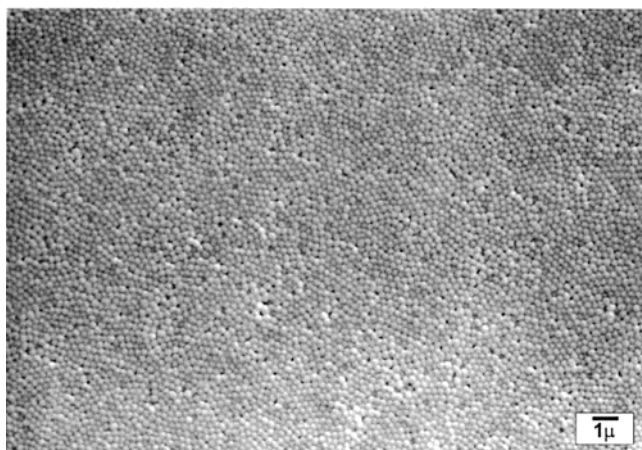


**Figure 8.** SEM picture of a colloidal crystal made from 250 nm silica spheres doped with CdSe/CdS nanocrystals (synthesized by the Stöber method).

of a film made from 250 nm silica spheres doped with CdSe/CdS nanocrystals. One to three micron domains with the fcc ordered colloidal crystal can be clearly observed, although the long-range order is quite limited due to the dispersion in sizes of silica spheres.

Colloidal crystals made from silica spheres are brightly colored in both transmitted and reflected light and exhibit opalescence (i.e., angle dependent coloration) because of the optical diffraction on regular multilayers. Optical transmission spectra of the samples show the existence of a photonic stop band (Figure 9). A shift of

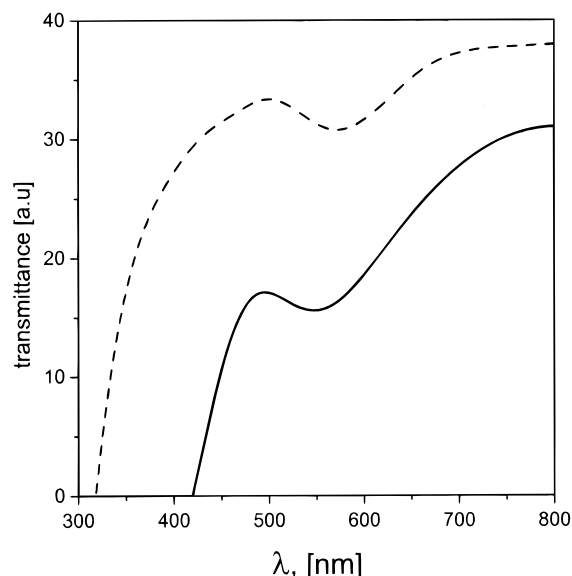


**Figure 9.** Transmission spectra of two colloidal crystals made from undoped silica spheres of 250 nm size grown by the Stöber method (solid line) and from silica spheres of the same size doped with CdSe/CdS nanocrystals (dashed line) showing the existence of photonic stop bands at different wavelengths.

the dip minimum to longer wavelengths of ca. 20 nm is observed for colloidal crystals made from CdSe/CdS-doped silica spheres in comparison with undoped ones.

### Discussion

Three types of water soluble semiconductor nanocrystals have been used for preparation of composite silica-semiconductor structures: CdSe, CdSe/CdS nanoparticles stabilized by citrate ions, and CdTe nanoparticles capped by thioglycerol. Citrate is known to be a relatively weak stabilizer ionically bound to the surface of inorganic colloids.<sup>13–15</sup> On the other hand, thiols are known to have a strong affinity for metal chalcogenides and to form covalent bonds on their surface. Interestingly, despite the bond strength, NMR experiments show that some equilibrium exists between the capping thiol molecules in solutions and that bound to the nanoparticle surface.<sup>51</sup>

The modification of nanocrystals with MPS as a primer was aimed to enhance the compatibility of nanoparticles with silicate, i.e., to make their surface vitreophilic. MPS molecules chemisorb to the nanocrystal surface at the Cd sites through their mercapto groups, whereas the siloxane groups are pointed out into the solution and hydrolyze quickly at pH 8.5.<sup>13</sup> The exchange of MPS with citrate ions has been shown to occur almost completely owing to their labile binding to the nanoparticle surface.<sup>13,14</sup> For CdTe nanocrystals whose surface is precapped with much stronger thioglycerol, the exchange of the stabilizer with MPS proceeds to a smaller extent than for citrate-capped nanocrystals. Nevertheless, the adsorption of some amount of MPS molecules on the nanoparticle surface can be suggested taking into account the dynamic nature of the thiol bonding.<sup>51,52</sup>

The modification of nanocrystals with MPS as well as a further silica coating using silicate has been carried

(50) Vlasov, Y.; Luterova, K.; Pelant, I.; Honerlage, B.; Astratov, V. N. *Thin Solid Films* **1998**, *318*, 93–95. Gaponenko, S. V.; Bogomolov, V. N.; Petrov, E. P.; Kapitonov, A. M.; Yarotsky, D. A.; Kalosha, I. I.; Eychmueller, A. A.; Rogach, A. L.; McGilp, J.; Woggon, U.; Gindele, F. *J. Lightwave Technol.* **1999**, *17*, 2128–2137. Holgado, M.; Garcia-Santamaria, F.; Blanco, A.; Ibisate, M.; Cintas, A.; Miguez, H.; Serna, C. J.; Molpeceres, C.; Requena, J.; Mifsud, A.; Meseguer, F.; Lopez, C. *Langmuir* **1999**, *15*, 4701–4704. Petrov, E. P.; Bogomolov, V. N.; Kalosha, I. I.; Gaponenko, S. V. *Acta Phys. Pol., A* **1998**, *94*, 761–771. Vlasov, Y.; Astratov, V. N.; Baryshev, A. V.; Kaplyanskii, A. A.; Karimov, O. Z.; Limonov, M. F. *Phys. Rev. E: Stat. Phys., Plasmas, Fluids, Relat. Interdiscip. Top.* **2000**, *61*, 5784–5793. Ballato, J.; James, A. *J. Am. Ceram. Soc.* **1999**, *82*, 2273–2275. Jethmalani, J. M.; Ford, W. T. *NATO ASI Ser., Ser. 3* **1996**, *18*, 477–484. van Blaaderen, A.; Rue, R.; Wiltzius, P. *Nature (London)* **1997**, *385*, 321–324. Jethmalani, J. M.; Ford, W. T. *Chem. Mater.* **1996**, *8*, 2138–2146. van Blaaderen, A.; Wiltzius, P. *Science (Washington, DC)* **1995**, *270*, 1177–1179. Verhaegh, N. A. M.; Blaaderen, A. v. *Langmuir* **1994**, *10*, 1427–1438.

(51) Hoppe, K. Diploma Thesis, University of Hamburg, 1997.



out in an ethanol–water mixture at a volume ratio of 4:1. The high percentage of ethanol in the reaction mixture was quite necessary because (1) MPS is much more soluble in ethanol than in water and (2) alcohol stimulates almost complete precipitation of the silicate onto the silanol-modified nanocrystals.<sup>14</sup> No polymerization of the hydrolyzed MPS molecules into amorphous silica on the first preparation stage has been observed under the experimental conditions used in this paper either from absorption and photoluminescence spectra of nanoparticles or from their TEM images. Therefore, We believe that the formation of “raisin buns” occurs because the addition of the silicate solution in alcohol-rich medium results in the quick condensation of silicate molecules to form silica spheres, which incorporate within them virtually anything that is present at the moment in the solution.<sup>12b</sup>

Polymerization of silica from the silicate solutions takes place on semiconductor nanocrystals using the silanol groups of hydrolyzed MPS as anchor points. As has been shown in ref 14 for Ag@SiO<sub>2</sub> composite structures, the silicate concentration of less than 0.01% and pH > 10 promote the formation of silica particles with multiple Ag dots. Conditions used for the polymerization of silicate in this paper (silicate concentration 0.005%, pH 10.7) also lead to the formation of silica spheres with numerous semiconductor nanocrystals being incorporated in bigger SiO<sub>2</sub> spheres.

Silica coverage of semiconductor nanocrystals alters their optical properties. Change of the refractive index of the surrounding medium leads to the observed broadening of the maxima of the first electronic transition in the absorption spectra (Figures 5a, 6a). Such broadening was also observed in refs 12,13 for the surface plasmon absorption band of gold nanoparticles covered by thick silica shells. Two other factors that may also contribute to the greater width of the absorption features are (1) an inhomogeneous effect of the silica coating in the position of energy levels in the nanoparticles and (2) possible alteration of particle size distribution caused by interfacial reactions on nanoparticles. The latter can also be seen as a strong blue shift of both absorption edge and luminescence band of CdTe nanoparticles incorporated in silica spheres (Figure 5). A possible reason could be the decrease of the size of the semiconductor core due to a partial oxidation of the nanocrystal surface during exchange of the stabilizer from thioglycerol to MPS. This can also explain the relative increase of the trapped emission from CdTe@SiO<sub>2</sub> structures (Figure 5b).

The Stöber synthesis,<sup>42</sup> that is, the hydrolysis of tetraethoxysilane in an alcoholic medium followed by the base-catalyzed polycondensation of silicic acid groups, typically leads to the formation of sufficiently monodisperse spherical silica particles with controlled sizes in the submicrometer region. Similar colloids (Figure 7) were obtained by the growth of nanoparticles-doped seeds (Figure 4). The modification of the basic Stöber reaction by using SiO<sub>2</sub> seeds affected the monodispersity of the particles and, therefore, requires further optimization to attain a slower rate of silica precipitation by varying the concentration media composition and pH.<sup>12b</sup>

Silica spheres made by the Stöber synthesis are widely used for the preparation of artificial opals, i.e.,

regularly packed 3D fcc colloidal crystals showing photonic band gap phenomenon.<sup>18–27</sup> The spectral position of the stop band in photonic crystals made from silica spheres depends on the period of the three-dimensional lattice, on the crystallographic orientation of the sample toward the direction of the incident light, and on the ratio of the refractive indices of the silica globules and the interglobule voids:<sup>24</sup>  $\lambda = 2nd$ , where  $n$  is the effective refractive index of the composite,  $n^2 = n_{\text{SiO}_2}^2 f + n_{\text{air}}^2(1 - f)$ ;  $f = 0.74$  is the filling factor for a close packed structure;  $d = 0.816\phi$ , the distance between crystalline planes in the direction  $\theta = 0^\circ$ ; and  $\phi$  is the sphere size. For the colloidal crystal made of pure silica with a diameter of 250 nm,  $n_{\text{SiO}_2} = 1.45$ , the peak photonic band gap is supposed to be at 550 nm. For the same opals, incorporating nanocrystals with filling factor of 0.05 (calculated from TEM),  $n_{\text{nanoparticle}} = 2.6$ , the peak position can be estimated to be 575 nm. In Figure 9, for pure opal the photonic band gap is observed at 561 nm, while for nanoparticle-doped opal it is seen at 573 nm. The position of both bands coincides quite well with the estimate, especially considering some uncertainty in determination of filling factor for the imperfect colloidal crystal. This allows us to attribute the observed dips in Figure 9 to the partial photonic band gap, which can be further substantiated by the strong opalescence. As was shown by Ballato et al.,<sup>53</sup> even imperfect colloidal crystals with limited long-range order are capable of demonstrating the spectral features of the photonic band gap. Our results corroborate with that conclusion. Another important observation pertaining to the effect of doping on photonic properties is the fact that the incorporation of semiconductor nanocrystals into silica particles leads to an increase of the effective refractive index of the composite which, in turn, shifts the position of the photonic stop band of colloidal crystals made thereof to the red (Figure 9).

## Conclusion

A synthetic method is developed for the preparation of “raisin-bun”-type composites of silica spheres with multiple cores of semiconductor nanocrystals. The method was tested for CdTe, CdSe, and CdSe/CdS nanoparticles capped with different organic stabilizers. The silica shell noticeably alters the optical properties of the nanoparticles due to (1) the change of the refraction index of the media, (2) the inhomogeneous broadening of the electronic transitions affected by the local morphology of the silica shell, and (3) the chemical reactions at the semiconductor/silica interface. The blue shift of the spectral features indicates the reduction of the particle size during the ripening of the silica layer. We have also demonstrated the possibility of organization of the well-separated single nanoparticles encapsulated in the silica colloids in the 3D structures exhibiting photonic band gap properties. The photonic band gap of such a crystal is shifted to the red as compared to the undoped colloidal crystal, which shows the feasibility of band gap tuning by altering the average refractive index of the spheres.

(52) Rockenberger, J.; Tröger, L.; Rogach, A. L.; Tischer, M.; Grundmann, M.; Eychmüller, A.; Weller, H. *J. Chem. Phys.* **1998**, *108*, 7807.

(53) Ballato, J.; Dimaio, J.; James, A.; Gulliver, E. *Appl. Phys. Lett.* **1999**, *75*, 1497–1499. Ballato, J. *J. Opt. Soc. Am. B* **2000**, *17*, 219–225.

In our opinion, the key direction for the optimization of the "raisin-bun" or similar silica/semiconductor composites is combating the reduction of the luminescence quantum yield observed after the formation of the silica shell.<sup>5</sup> Recently, the feasibility of double-digit percent luminescence quantum yield for nanoparticles/silica composite made from CdSe/CdS stabilized by citrate was demonstrated in the new series of experiments done in collaboration with Liz-Marzan's group.<sup>54</sup> The results of this study will be the subject of subsequent publication(s).

Finally, as one reviewer of the manuscript pointed out, the "raisin-bun" composite is reminiscent of the "plum-pudding" model of atom suggested by J. J. Thomson in 1906. Although we used this term only for descriptive purposes without deliberate allusion to the

---

(54) Correa-Duarte, M.; Nagesha, D.; Kotov, N. A.; Liz-Marzan, L. M.; unpublished results.

atomic model, the preparation of a 3D crystal from such scaled-up 250 nm "atoms" lends some validity to this analogy.

**Acknowledgment.** A.L.R. and N.A.K. acknowledge the support of the National Research Council (COBASE grants program) that made collaborative work on this project possible. N.A.K. also acknowledges the partial support of this research from an NSF-CAREER (CHE-9876265) award. A.L.R. is indebted to INTAS for the research grant INTAS-Belarus 97-250. We thank ORNL for research grant (00\_KotovNA\_01) and Dr. E. Kenik and Dr. N. Evans from the ORNL for the help with TEM images. N.A.K. particularly thanks Dr. L. M. Liz-Marzán from the University of Vigo for numerous stimulating discussions and insights. All authors would like to thank the reviewers for useful comments.

CM000244I